HHS Public Access

Author manuscript

Nano Lett. Author manuscript; available in PMC 2019 March 28.

Published in final edited form as:

Nano Lett. 2006 March ; 6(3): 371–375. doi:10.1021/nl051829k.

Detection of DNA Hybridization using the Near Infrared Band-gap Fluorescence of Single-Walled Carbon Nanotubes

Esther S. Jeng, **Anthonie E. Moll**, **Amanda C. Roy**, **Joseph B. Gastala**, and **Michael S. Strano***

Department of Chemical and Biomolecular Engineering, University of Illinois-Urbana/Champaign, 600 S. Mathews Avenue, Urbana, Illinois 61801, USA

Abstract

We demonstrate the optical detection of DNA hybridization on the surface of solution suspended single-walled carbon nanotubes (SWNT) through a SWNT band gap fluorescence modulation. Hybridization of a 24-mer oligonucleotide sequence with its complement produces a hypsochromic shift of 2meV, with a detection sensitivity of 6 nM. The energy shift is modeled by correlating the surface coverage of DNA on SWNT to the exciton binding energy, yielding an estimated initial fractional coverage of 0.25, and a final coverage of 0.5. Hybridization on the nanotube surface is confirmed using FRET of fluorophore labeled DNA oligonucleotides. This detection is enabled through a new technique to suspend SWNT using adsorption of single-stranded DNA and subsequent removal of free DNA from solution. While the kinetics of free DNA hybridization are relatively fast (< 10min), the kinetics of the process on SWNT are slower under comparable conditions, reaching steady state after 13 hours at 25 °C. A second order kinetic model yields a rate constant of k=4.33×10^5 (M-hr)$^{-1}$. This optical, selective detection of specific DNA sequences may have applications in the life sciences and medicine as in-vitro or in-vivo detectors of oligonucleotides.

Detection of specific single stranded DNA sequences through hybridization with the complementary DNA probe has many applications in the medical and life sciences[1–3], environmental science[4,5], and microbiology[6–9]. Hybridization detection techniques include surface sensors[10,11], used for ultra-low concentration detection, and solution based sensors[12,13], that are used for direct detection in biological systems. The use of fluorescence, specifically for detection in the solution based systems, is advantageous due to the sensitivity and selectivity of the technique[14]. Previous fluorescence sensors have included DNA chips[8,15], molecular beacons[12], and the use of Forster Resonance Energy Transfer[13].

Individually dispersed semiconducting single walled carbon nanotubes (SWNT) are excellent candidates for optical sensors, as we have shown previously[16]. Because SWNT fluoresce at near infrared (nIR) wavelengths[17,18], they have the potential to be used in biological applications due to the low absorption of blood and tissue[17–19], and the low autofluorescence of cells[20] in the nIR. Furthermore, SWNT are sensitive to molecular adsorption at their surface[16,21] and are resistant to photobleaching[22]. SWNT can be

* strano@uiuc.edu.

individually dispersed by adsorbing molecules to the nanotube surface in solution, eliminating the need for fluorescent labels and dyes[16,23–25]. Some DNA sequences have been shown to adsorb strongly to the surface of nanotubes resulting in a stable suspension[25,26]. Nanotubes have also been successfully implanted in cells [27,28], allowing for potential *in vivo* applications as we[22,27,28] and others have shown[22,27,28].

In this work, we show the first photobleaching resistant, nanoparticle system that allows for the detection of DNA hybridization through the modulation of a near-infrared fluorescence signal from a DNA-SWNT complex. In separate experiments, the hybridization events are confirmed through Forster Resonance Energy Transfer (FRET) by studying the visible fluorescence signal of fluorophore labeled DNA-SWNT with the addition of the fluorescently tagged complement. This is the first work to optically detect selective hybridization of DNA with its complementary strand directly on the surface of SWNT, and therefore opens possibilities for new types of nanotube-based molecular beacons, sensors, probes and sequencing technologies.

We developed a novel method to directly suspend SWNT with single-stranded DNA (ssDNA), and remove free ssDNA, as illustrated in fig. 1. Single walled HiPCO carbon nanotubes from the Rice University Research Reactor (run 107) were individually dispersed in 2 wt% sodium cholate (Sigma Aldrich) in nanopure water in a method we have outlined previously.[16,17] DNA (5’ – TAG CTA TGG AAT TCC TCG TAG GCA – 3’) was assembled on the surface of the SWNT through dialysis against standard Tris buffer of the cholate SWNT in the presence of DNA in a method discussed previously[16].

The spectra of the cholate-SWNT and DNA-SWNT in figure 1 show that a bathochromic shift of 17.6 meV (15.6nm) occurs for the (7,5) tube when the cholate molecules are replaced by DNA oligonucleotides, which is greater than the shift observed in the previous Glucose Oxidase system that we studied[16]. The red shift is caused by the sparser DNA coverage on the SWNT surface as compared to the smaller, more densely packed, cholate molecules. The greater exposed area on the SWNT increases contact with water, resulting in a decrease in the SWNT emission energy.[24] The free DNA in solution was removed through a 2nd stage, high molecular weight dialysis in order to ensure that hybridization occurred on the SWNT surface and potential artifacts from hybridization of free DNA were minimized. Dialysis for 48 hours removed 95% of the free DNA as determined by UV-visible absorption spectroscopy. The final concentrations of SWNT and DNA in solution were estimated to be 27 nM and 118 nM, respectively, using absorption spectroscopy. The residual concentration of the sodium cholate was calculated to be 4.5pM.

We find that hybridization of the DNA strands with their complements (cDNA 5’- GCC TAC GAG GAA TTC CAT AGC T – 3’) adsorbed on the SWNT surface is transduced by a hypsochromic shift in the near infrared fluorescence of the SWNT. The (6,5) nanotube fluorescence (λ_{max}=994nm) was monitored with a laser excitation of 785nm[29,30]. DNA-SWNT was incubated for 48 hours with different concentrations of cDNA and non-complementary DNA (nDNA 5’ - TCG ATA CCT TAA GGA GCA TCC G −3’) to ensure that steady state was reached. The energy of the (6,5) peak increases up to 2.02±0.07 meV with the addition of cDNA, indicating a decrease in the effective dielectric constant of the

SWNT environment, which we interpret as a denser surface coverage after hybridization (Fig. 2). In contrast, the addition of nDNA does not result in any significant shift. This selectivity of the energy shift indicates that DNA hybridization is occurring on the nanotube surface. Sample spectra of the (6,5) fluorescence peaks with and without cDNA are shown in figure 2b.

The observed energy shift, E, can be explained as an increase in the exciton binding energy caused by an increase in the surface area coverage of the SWNT. Using an effective medium approximation, the local dielectric constant, s, at the SWNT surface is:

$$\varepsilon = \alpha\varepsilon_{DNA} + (1-\alpha)\varepsilon_{H_2O}$$

Where α is the fraction of SWNT surface area covered by DNA, and ε_{DNA}=2.1, ε_{H2O}=88 represent the dielectric constants of DNA and water respectively. The sodium cholate concentration was considered too small to significantly affect the dielectric constant. A simplified variational model[31] is used to correlate the exciton binding energy change to the fraction of unexposed SWNT surface area. The exciton binding energy, E (eV), can be calculated as a function of the local dielectric constant with the following relation:

$$E = -\frac{R\mu}{\varepsilon^2 K}\left(\frac{1}{K} + 4\left[\gamma + \ln\left(\frac{\mu r}{\beta\varepsilon K}\right)\right]\right)$$

Where R=13.6eV is the Ryberg conversion factor, μ=0.068 is the reduced effective mass of the (6,5) nanotube[18], r=0.4nm is the radius of the (6,5) nanotube, K=2.28 is a variational parameter specific to the (6,5) tube that is adjusted to minimize the energy, γ=0.577 is the Euler constant, and β=0.0529 nm is the Bohr radius constant.

Saturation of the SWNT surface caused a 2.02±0.07 meV change, as shown in fig. 2 and this should correspond to an approximate doubling of SWNT surface coverage from the DNA hybridization. By fixing these two degrees of freedom, the model predicts that the initial coverage of DNA is 25%, while the saturation coverage is 50%. In this range, the model is roughly linear, as are the energy shifts we observe during hybridization. The fractional coverage was converted to concentrations of cDNA and the model is shown in fig. 2. Beyond the DNA saturation point, the energy is assumed to remain constant (fig. 2).

DNA hybridization on SWNT was confirmed in a separate study using Forster Resonance Energy Transfer (FRET) between fluorescently labeled DNA strands. The 3’ end of the DNA was tagged with a fluorescein derivative, FAM™, which serves as the donor. This tagged DNA was assembled on the SWNT surface in the method outlined above, to synthesize DNA-D-SWNT. Complementary DNA strands (cDNA-A) with 5’ attached acceptor fluorophores, TAMRA™ NHS Ester, were added to the DNA suspended SWNT over a concentration range of 33–350 nM. The experiment was repeated using non-complementary strands of DNA conjugated to the same acceptor fluorophore (nDNA-A) as a control. In order to confirm that there was a negligible amount of free DNA in solution, the emission of dialyzed free DNA-D (3.13×10^4) was compared to the emission of the dialyzed

DNA-D-SWNT (8.45×10^4), both of which are significantly smaller than the emission of the free DNA-D before dialysis, 1.18×10^7 The SWNT is shown to quench the fluorophore, as is seen in the comparison of the donor emission of free and SWNT-adsorbed DNA[32]. Therefore the amount of free DNA in solution is considered to be negligible compared to the amount of DNA on the nanotube.

The significant decrease in the donor emission within 2 minutes of the first addition (33nM) of cDNA-A to the DNA-D-SWNT solution indicates FRET and therefore hybridization. In contrast, the addition of nDNA actually increases the donor emission at higher concentration (fig. 3b,d). Subsequent additions of cDNA-A resulted in a further decrease in donor emission until the cDNA-A concentration reached 127 nM, where the donor fluorescence began to increase slightly. However, the donor fluorescence remained significantly lower in the presence of cDNA-A than without it (fig. 3a,c).

Although not central to this study, we note that the increase in donor emission (fig. 3a) indicates that some of the donor fluorophores are no longer within 0.5–5nm of the nanotube and are unquenched (see supplement). Additions of nDNA-A to the DNA- D-SWNT solution also result in an increase in donor emission. The origin of this increase in both cases is currently under investigation. One possible mechanism is that DNA-D undergoes a change in conformation in response to hybridization with cDNA-A or repulsion from nDNA-A. In this case, the fluorophore end extends from the nanotube and is then unquenched, while the remaining DNA is still adsorbed to the SWNT. Another possibility is that the nDNA-A is replacing the DNA-D completely on the SWNT surface.

The total number of binding sites for DNA on SWNT was estimated to be of order 50/SWNT based on the dimensions of the two molecules. The SWNT are approximately 1 μm long with diameters between 0.6 and 1.3 nm, and the oligonucleotides used in this work are approximately 10 nm long with an estimated repulsion distance of 5 nm[33].

We find that the kinetics of these hybridization events are exceedingly slow at 25°C on the nanotube surface compared to the rate for free DNA in solution. The transient response of the SWNT fluorescence with cDNA and nDNA additions was monitored at room temperature to measure the amount of time necessary for the hybridization peak shift to reach steady state (fig. 4). For a concentration of 625nM cDNA, approximately 13 hours are required for the hybridization reaction to reach steady state, although our FRET study indicates that hybridization occurs within minutes. The addition of nDNA does not result in a significant response. The standard deviation of 0.03 meV of the steady state peak energy over 9 hours was also used to determine the mean noise level and yields an approximate hybridization detection limit for cDNA concentrations as low as 6nM. The rate of the SWNT fluorescence energy change was modeled using the following mechanism:

$$\underset{DNA}{A} + \underset{cDNA}{B} \xrightarrow{k} \underset{Hybridized\_Complex}{H}$$

The rate of formation of the hybridized complex was modeled using this second order reaction, in accordance with the known kinetic behavior of unbound DNA hybridization[34].

$$\frac{dC_H}{dt} = kC_A C_B$$

The time is t (hr), k is the kinetic constant (M-hr)$^{-1}$, and C_A, C_B, and C_H are the concentrations (M) of DNA adsorbed to SWNT, complementary DNA, and hybridized DNA on SWNT, respectively. After solving the differential equation, the concentration of the hybridized complex at any given time can be calculated using the equation:

$$C_{H(t)} = C_{A0} + \frac{C_{A0}(C_{A0} - C_{B0})}{-C_{A0} + C_{B0}\exp[(C_{B0} - C_{A0})kt]}$$

where C_{A0} is the initial concentration of DNA (118nM) that is adsorbed to the SWNT and C_{B0} is the initial concentration of complement added to the system. This equation was used to fit the fluorescence energy shift by correlating the normalized concentration of hybridized complex to the normalized energy change:

$$\frac{C_H}{C_{H,\max}} = \frac{\Delta E}{\Delta E_{\max}}$$

where $C_{H,max} = C_{A0}$ represents hybridization of every adsorbed DNA strand, and ΔE_{max} (2meV) is the maximum energy shift observed at saturation conditions. The model is shown in figure 4 as a solid line, with k=4.33×10^5 (M-hr)$^{-1}$. DNA is known to hybridize in fewer than 10 min[35], and the addition of salts such as MgCl2 stabilize[12] and speed up hybridization[36], due to the ionic shielding of the ions. Further kinetic investigations involving ionic strength of various salts and temperature will be conducted to probe the effects on the SWNT system.

This system has the potential to be used in studying low copy DNA hybridization, and in similar biological assays. Efforts to use DNA for directed assembly of SWNT will also benefit from this optical detection. More importantly, there may be applications of these new types of sensors to the life sciences and medicine since SWNT near infrared fluorescence is optimized for tissue penetration, photostability and the avoidance of biological auto-fluorescence.

Conclusions.

We conclude from our results that the hybridization of DNA can be detected using the optical modulation of the SWNT n-IR fluorescence, and has a calculated detection limit of 6 nM DNA. The observed energy change of 2meV from the DNA hybridization is well described by an effective medium dielectric model, indicating that an initial DNA surface coverage of 25% increases to 50% after hybridization on the SWNT. The total number of binding sites for DNA is estimated to be 50sites/SWNT, based on the dimensions of the DNA and SWNT. The hybridization event at the nanotube surface is also confirmed using FRET. The kinetics of hybridization on the SWNT were modeled used a second order

reaction, yielding a kinetic constant of k=4.33×10^5 (M-hr)$^{-1}$. Hybridization of free DNA is fast (<2min), but the transduction process is considerably slower on SWNT (13hours). Further investigation will elucidate the reason for this discrepancy.

Materials.

Dialysis of cholate SWNT was done with a Slide-A-Lyzer Dialysis Cassette 10kDa MWCO (Pierce Biotechnology, Inc.) while the free DNA was removed using Spectra/Por Biotech CE membranes (100kDa MWCO) (Spectrum Laboratories)

The fluorophore tagged DNA sequence used to suspend SWNT is 5’ – TAG CTA TGG AAT TCC TCG TAG GCA – 3’ – 6-FAM™, the cDNA sequence with fluorophore is TAMRA™ NHS Ester -- 5’- GCC TAC GAG GAA TTC CAT AGC T – 3’, and the nDNA sequence with fluorophore is TAMRA™ NHS Ester -- 5’- TCG ATA CCT TAA GGA GCA TCC G −3’. All of the sequences were purchased from Integrated DNA Technologies, Inc.

Supplementary Material

Refer to Web version on PubMed Central for supplementary material.

Acknowledgements.

The authors acknowledge the National Science Foundation (grant no. CTS-0330350). M.S.S is grateful for a 2004 Dupont Young Investigator Award. FRET experiments were conducted at the Laboratory for Fluorescence Dynamics (LFD) at the University of Illinois at Urbana-Champaign (UIUC), which is supported jointly by the National Center for Research Resources of the National Institutes of Health (PHS 5 P41-RR003155) and UIUC. We acknowledge graduate students P.W. Barone and D.A. Heller for helpful discussions.

References

(1). Nolte FS; Metchock B; McGowan JE; Edwards A; Okwumabua O; Thurmond C; Mitchell PS; Plikaytis B; Shinnick T Journal of Clinical Microbiology 1993, 31, 1777–1782. [PubMed: 8349753]

(2). Hamiltondutoit SJ; Pallesen G; Franzmann MB; Karkov J; Black F; Skinhoj P; Pedersen C American Journal of Pathology 1991, 138, 149–163. [PubMed: 1846263]

(3). Senda K; Arakawa Y; Nakashima K; Ito H; Ichiyama S; Shimokata K; Kato N; Ohta M Antimicrobial Agents and Chemotherapy 1996, 40, 349–353. [PubMed: 8834878]

(4). Louws FJ; Fulbright DW; Stephens CT; Debruijn FJ Applied and Environmental Microbiology 1994, 60, 2286–2295. [PubMed: 8074510]

(5). Juretschko S; Timmermann G; Schmid M; Schleifer KH; Pommerening- Roser A; Koops HP; Wagner M Applied and Environmental Microbiology 1998, 64, 3042–3051. [PubMed: 9687471]

(6). Wei Y; Lee JM; Richmond C; Blattner FR; Rafalski JA; LaRossa RA Journal of Bacteriology 2001, 183, 545–556. [PubMed: 11133948]

(7). Kuykendall LD; Saxena B; Devine TE; Udell SE Canadian Journal of Microbiology 1992, 38, 501–505.

(8). Heller MJ Annual Review of Biomedical Engineering 2002, 4, 129–153.

(9). Pease AC; Solas D; Sullivan EJ; Cronin MT; Holmes CP; Fodor SPA Proceedings of the National Academy of Sciences of the United States of America 1994, 91, 5022–5026. [PubMed: 8197176]

(10). He L; Musick MD; Nicewarner SR; Salinas FG; Benkovic SJ; Natan MJ; Keating CD Journal of the American Chemical Society 2000, 122, 9071–9077.

(11). Park SJ; Taton TA; Mirkin CA Science 2002, 295, 1503–1506. [PubMed: 11859188]

(12). Tyagi S; Kramer FR Nature Biotechnology 1996, 14, 303–308.

(13). Gaylord BS; Heeger AJ; Bazan GC Journal of the American Chemical Society 2003, 125, 896–900. [PubMed: 12537486]

(14). Kumke MU; Li G; McGown LB; Walker GT; Linn CP Analytical Chemistry 1995, 67, 3945–3951. [PubMed: 8633758]

(15). Southern EM Trends in Genetics 1996, 12, 110–115. [PubMed: 8868349]

(16). Barone PW; Baik S; Heller DA; Strano MS Nature Materials 2005, 4, 86–92. [PubMed: 15592477]

(17). O'Connell MJ; Bachilo SM; Huffman CB; Moore VC; Strano MS; Haroz EH; Rialon KL; Boul PJ; Noon WH; Kittrell C; Ma JP; Hauge RH; Weisman RB; Smalley RE Science 2002, 297, 593–596. [PubMed: 12142535]

(18). Bachilo SM; Strano MS; Kittrell C; Hauge RH; Smalley RE; Weisman RB Science 2002, 298, 2361–2366. [PubMed: 12459549]

(19). Wray S; Cope M; Delpy DT; Wyatt JS; Reynolds EOR Biochimica Et Biophysica Acta 1988, 933, 184–192. [PubMed: 2831976]

(20). Weissleder R. a. N.V Nature Medicine 2003, 9, 123–128.

(21). Saito R, Dresselhaus G & Dresselhaus MS Physical Properties of Carbon Nanotubes; Imperial College Press: London, 1998.

(22). Heller D; Baik S; Eurell T; Strano M Advanced Materials 2005, advanced publication online.

(23). Moore VC; Strano MS; Haroz EH; Hauge RH; Smalley RE; Schmidt J; Talmon Y Nano Letters 2003, 3, 1379–1382.

(24). Strano MS; Moore VC; Miller MK; Allen MJ; Haroz EH; Kittrell C; Hauge RH; Smalley RE Journal of Nanoscience and Nanotechnology 2003, 3 81–86. [PubMed: 12908233]

(25). Zheng M; Jagota A; Strano MS; Santos AP; Barone P; Chou SG; Diner BA; Dresselhaus MS; McLean RS; Onoa GB; Samsonidze GG; Semke ED; Usrey M; Walls DJ Science 2003, 302, 1545–1548. [PubMed: 14645843]

(26). Strano MS; Zheng M; Jagota A; Onoa GB; Heller DA; Barone PW; Usrey ML Nano Letters 2004, 4, 543–550.

(27). Singh R; Pantarotto D; McCarthy D; Chaloin O; Hoebeke J; Partidos CD; Briand JP; Prato M; Bianco A; Kostarelos K Journal of the American Chemical Society 2005, 127, 4388–4396. [PubMed: 15783221]

(28). Cherukuri P; Bachilo SM; Litovsky SH; Weisman RB Journal of the American Chemical Society 2004, 126, 15638–15639. [PubMed: 15571374]

(29). Strano MS; Doorn SK; Haroz EH; Kittrell C; Hauge RH; Smalley R Nano Letters 2003, 3, 1091–1096.

(30). Dresselhaus MS; Dresselhaus G; Saito R Carbon 1995, 33, 883–891.

(31). Pedersen TG Physical Review B 2003, 67.

(32). Supplemental Information

(33). Mariani P; Ciuchi F; Saturni L Biophysical Journal 1998, 74, 430–435. [PubMed: 9449343]

(34). Wetmur J. G. a. D. Norman Journal of Molecular Biology 1968, 31, 325–633.

(35). Ferguson JA; Boles TC; Adams CP; Walt DR Nature Biotechnology 1996, 14, 1681–1684.

(36). Liu XJ; Farmerie W; Schuster S; Tan WH Analytical Biochemistry 2000, 283, 56–63. [PubMed: 10929808]

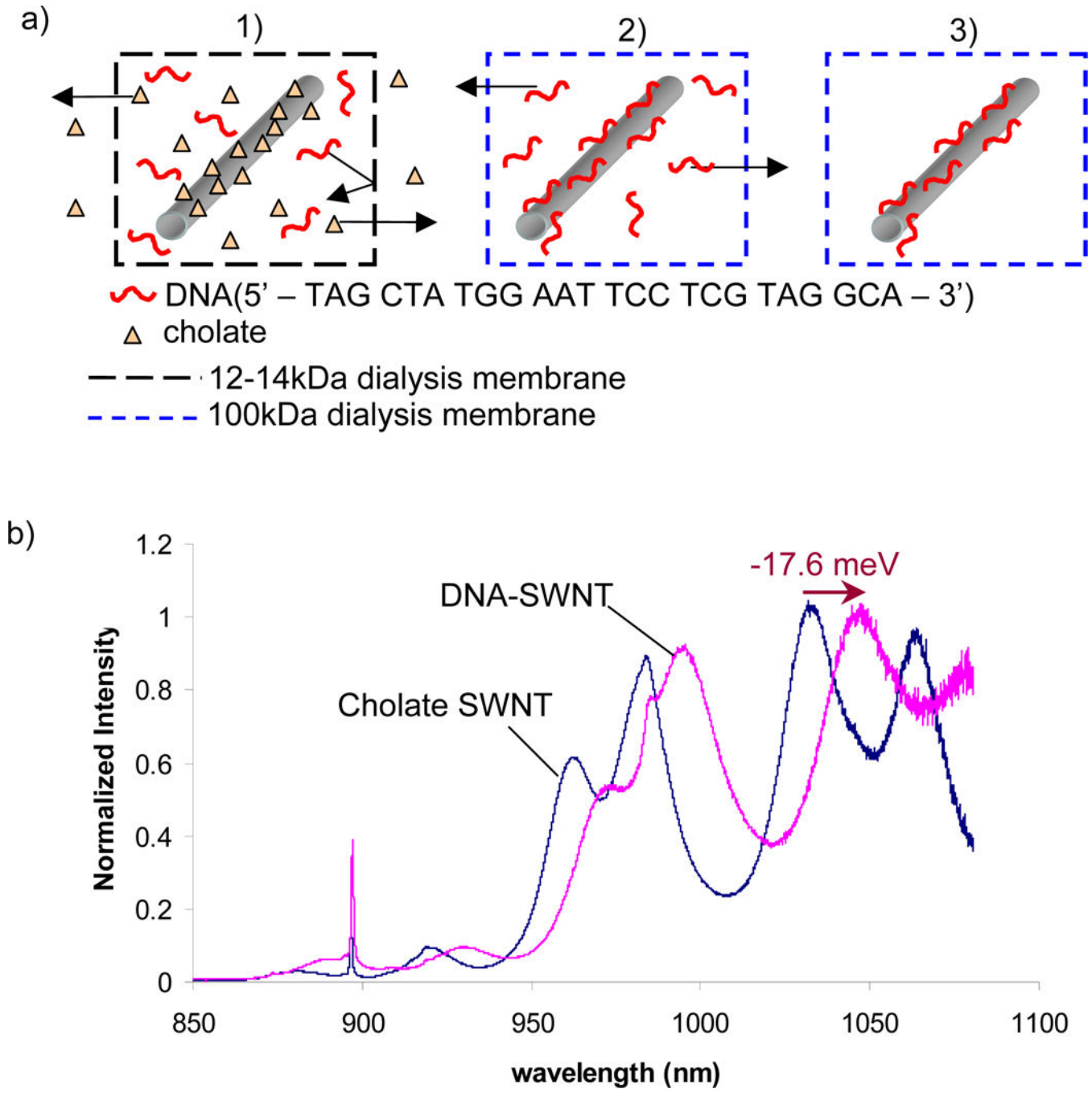

Figure 1:

Synthesis of DNA-SWNT: a) diagram of the suspension process in lXTris buffer 1) Dialysis of cholate suspended SWNT with DNA (12–14kDa dialysis bag) 2) Dialysis of free DNA (100kDa MWCO dialysis bag) 3) DNA-SWNT with no free DNA b) Combined Raman and nIR fluorescence spectra indicate significant red shifting of DNA-SWNT fluorescence as compared to the fluorescence of cholate SWNT

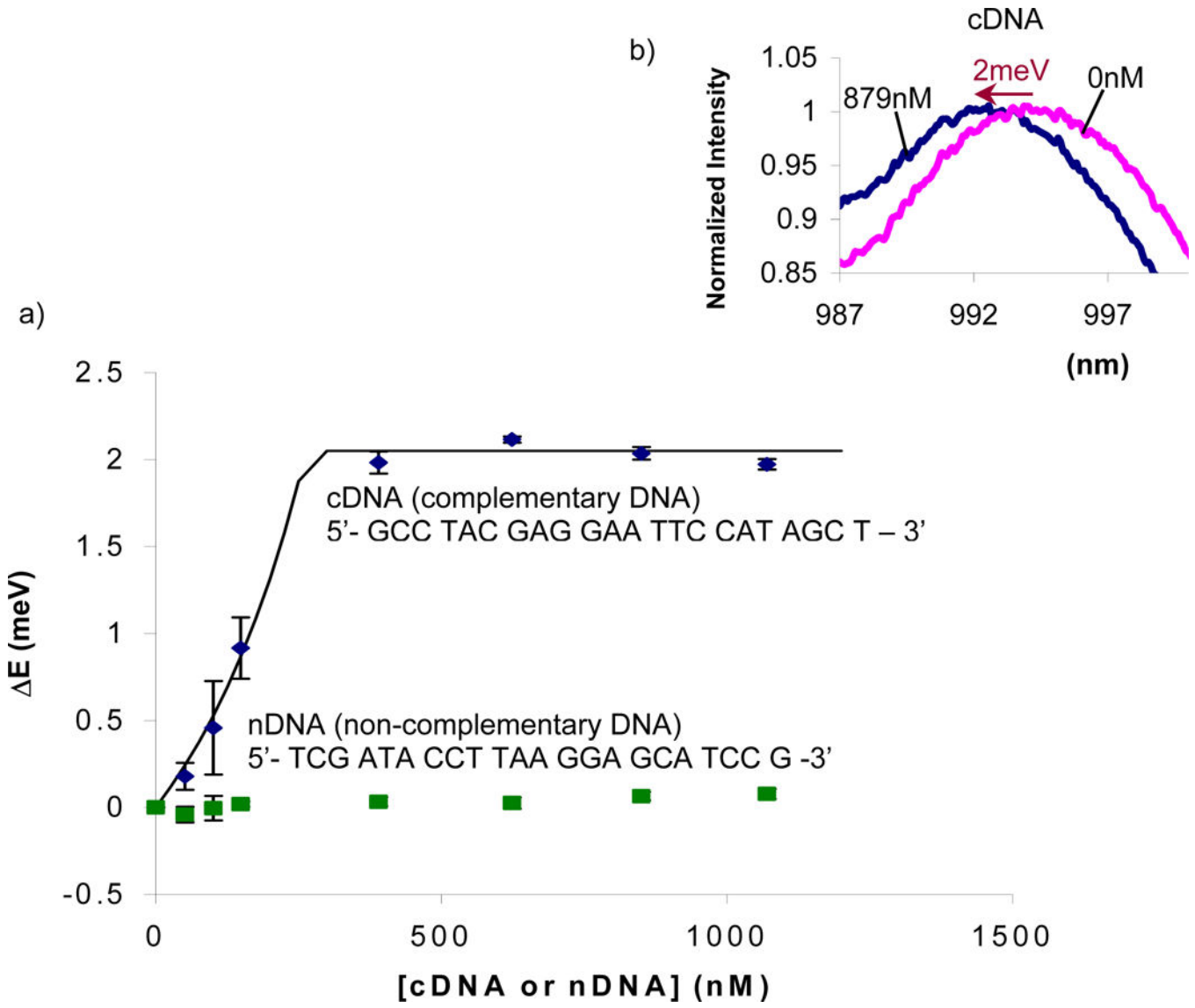

Figure2:

a) Addition of complementary DNA (cDNA) causes an increase in energy of the steady state (6,5) fluorescence peak while there is negligible energy change with non-complementary DNA (nDNA). The solid line is a fit of the dielectric model to the cDNA energy shifts. b) Sample spectra of the fluorescence peak blue shift with cDNA addition.

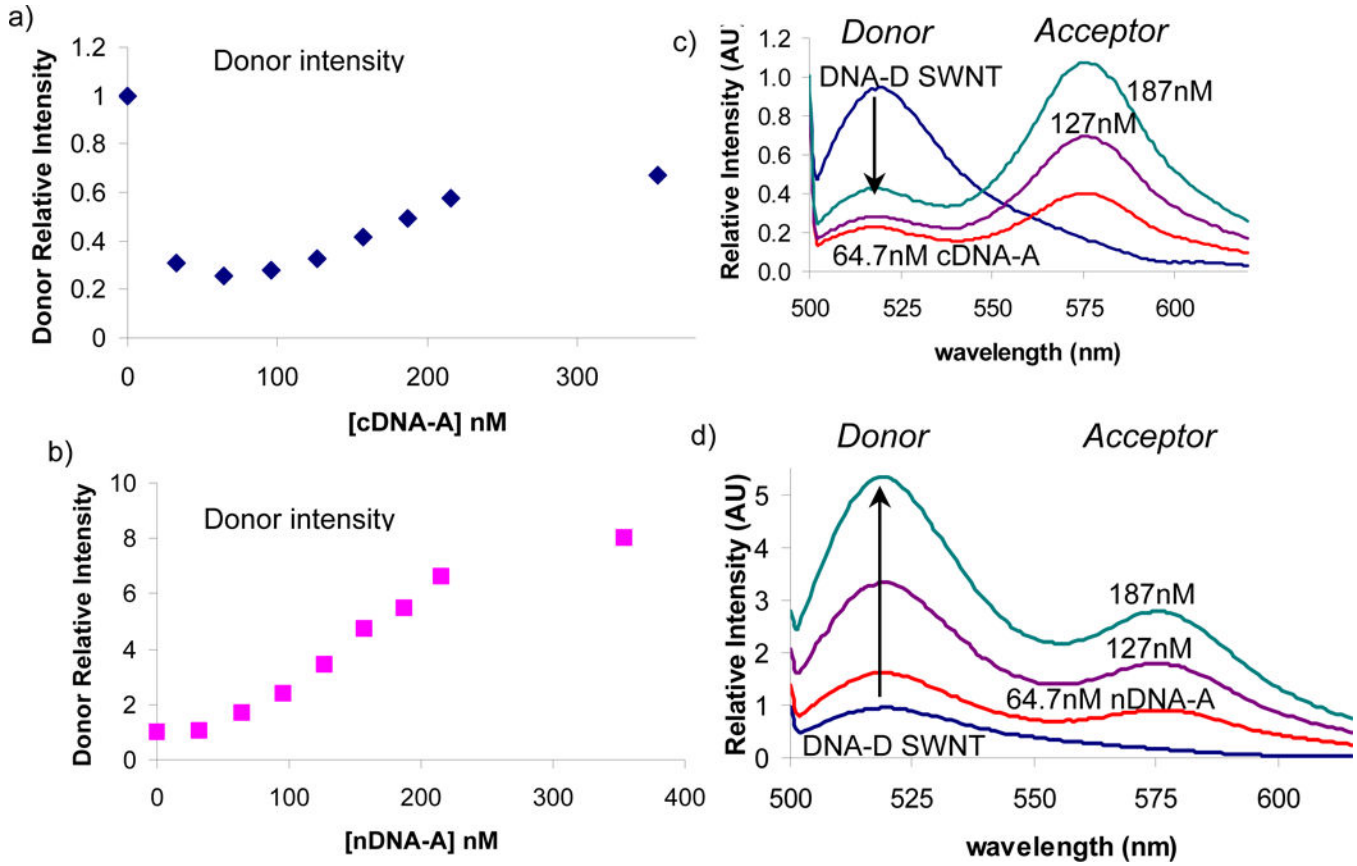

Figure 3:

Intensity at donor emission (max 520nm) of DNA-D SWNT a) Additions of complement conjugated with acceptor (cDNA-A) result in decrease of donor emission at concentrations <127nM, then partial recovery of donor emission at concentrations >127nM. b) Additions of non-complement conjugated with acceptor (nDNA-A) result in constant increase of donor emission. c) Forster resonance energy transfer (FRET) indicates DNA hybridization on nanotube surface. Emission of donor on DNA-D-SWNT decreases with additions of cDNA-A (attached to acceptor). d) No FRET between donor (DNA SWNT) and acceptor (nDNA) indicate that there is no hybridization occurring.

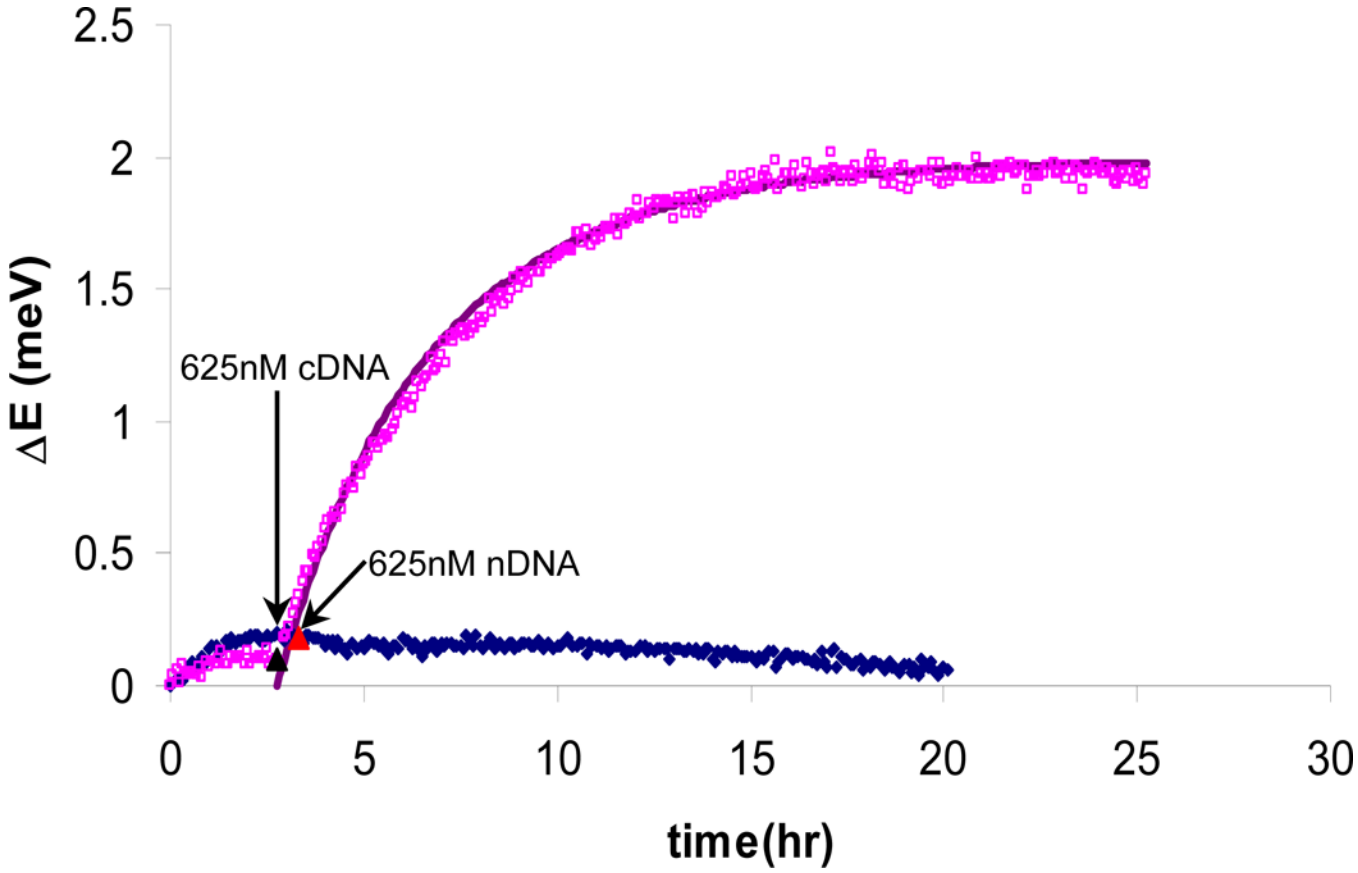

Figure 4:

Investigation of (6,5) peak shift kinetics at room temperature. The hybridization configuration of DNA-SWNT with cDNA requires approximately 13 hours to reach steady state while the addition of nDNA does not result in any significant peak shifting. The kinetics model is denoted by the solid line and has k=4.33×10^5 (M-hr)$^{-1}$.